Effect of Temperature on Zirconia Powder Synthesized from Amang Zirconium Oxychloride Precursor

Nur Fatinhanani Fatimah Norsham[1], Istikamah Subuki[2,*]

1   School of Chemical Engineering, College of Engineering, Universiti Teknologi MARA, 40450 Shah Alam, Selangor, Malaysia
2   Circular + Industrial Research Laboratory, School of Chemical Engineering, College of Engineering, Universiti Teknologi MARA, 40450 Shah Alam, Selangor, Malaysia

ARTICLE INFO

ABSTRACT

Polymorphic zirconia is economically attractive in various applications due to its low reactivity, high strength, and stability. Zirconia can be synthesized from locally available Amang zircon sand as an inexpensive green alternative as it has a high zirconium content as reported by previous report. Unfortunately, the study was only focused on the formation of zirconium oxychloride despite of high zirconium content from the improved alkali fusion method proposed. Therefore, a further study on zirconia powder calcined in varied temperatures from Amang zirconium oxychloride precursor was done. Amang zirconia powder was then characterized in order to study the effect of temperature on Amang zirconia powder. Elemental analysis showed that zirconium composition was affected by temperature and increased as the temperature increased with the highest zirconium content of 81.28 wt.% with low impurities after calcined at 800 °C for 4 hours. The phase analysis satisfied monoclinic zirconia with minor tetragonal and cubic phase with sharper peaks as calcined temperature increased. Increased tetragonal and cubic phase was observed as the temperature was increased. Morphology analysis showed zirconia powder was angular and pyramidal with large crystal size which led to high tendency of monoclinic phase. Calcination temperature of 800 °C was determined to be the most suitable temperature to calcine high purity zirconia powder using Amang zirconium oxychloride precursor.

1. Introduction

Zirconia is a polymorphic material suitable to be used in many fields such as in dentistry, aerospace, optical ceramic, and glaze coating due to its excellent properties [1-3]. It has high melting and boiling points, low thermal conductivity, inert and unreactive [4]. Zirconia also has a high abrasion resistance, high refractive index and dielectric constant [5,6]. Zirconia is also cheaper and has a higher melting point than alumina [7].

Depending on temperature, zirconia is available in monoclinic, tetragonal and cubic phases [8]. Monoclinic zirconia is thermodynamically stable at room temperature and up to 1170 °C [9]. A strong

---

covalent bond exists between zirconium and hepta-coordinated oxygen atoms in monoclinic phase [10]. Monoclinic zirconia shows a high resistance to cracking and exhibits outstanding properties. Monoclinic zirconia will then transform to octa-coordinated tetragonal at 1170 °C to 2370 °C [11]. This phase transformation improved the mechanical properties of zirconia. However, pure tetragonal zirconia is highly unstable at room temperature [12]. Octa-coordinated cubic zirconia is stable at temperatures higher than 2370 °C [11,12]. Like tetragonal zirconia, cubic zirconia cannot maintain its phase at room temperature.

Zirconia can be synthesized using zirconium oxychloride precursor from zircon sand. Zircon sand also known as zirconium silicate is a gold-colored mineral that typically contains high amount of zirconium, silicon and traces of other elements [13-15]. The wide availability of zirconium in zircon sand makes it the dominant source for zirconia. In Malaysia, zircon is found in the tin tailing produced by the tin mining industry, also known as Amang.

Alkali fusion with sodium hydroxide (NaOH) is typically used to synthesize zirconia from zircon sand as the calcination temperature can be lowered until 600 °C compared to other method that need a very high temperature to synthesize a high purity zirconia [16]. Consequentially, higher production cost results in a poor economic benefit [17]. Zircon and sodium hydroxide decomposition was typically done in according to Eq. (1):

$$ZrSiO_4 + 4NaOH \rightarrow Na_2ZrO_3 + Na_2SiO_3 + 2H_2O \qquad (1)$$

Zirconia from zircon sand has been synthesized in Brazil. However, the research was only done until zirconyl sulphate and no further synthetization was reported. Conversely, a study from Indonesian zircon sand by Lestari *et al.,* [18], had successful synthesized monoclinic and tetragonal zirconia using a high calcination temperature of 1300 °C. The research also observed that calcination temperature highly affects zirconia composition.

As for Amang zircon sand, a research was done previously using alkali fusion method that has been improved with 6M sodium hydroxide (NaOH) and 8M hydrochloric acid (HCl) [19]. The improved method produced a higher zirconium content with lower silica impurity. However, the research was only done up until zirconium oxychloride despite it can be used as a low-cost alternative to synthesis a high purity zirconia by manipulating the temperature during calcination process.

Therefore, Amang zirconium oxychloride from the improved alkali fusion method by Subuki *et al.,* [19] was used as a precursor to synthesize zirconia powder in varied temperatures. The effect of temperature on zirconia powder was studied to determine the effectiveness of the improved alkali fusion method to synthesize a high purity zirconia powder. Hence, improving and utilizing the local Amang zircon sand and reducing the accumulation of Amang zircon sand.

2. Methodology

The purpose of this research is to study the effect of temperature on zirconia powder synthesized from Amang zirconium oxychloride precursor. Therefore, synthetization of zirconia powder in varied temperatures using improved alkali fusion method was studied.

2.1 Materials and Chemicals

Amang zirconium oxychloride ($ZrOCl_2.8H_2O$) obtained from raw Amang zircon sand using improved alkali fusion method was used as a precursor to synthesize zirconia powder. Analytical grade of 25% ammonia solution (NH_4OH) from R&M Chemicals was used to precipitate zirconium

while pure water and 95% ethyl alcohol from Systerm were used to synthesize zirconia powder in this research.

2.2 Method

Zirconia powder was synthesized using Amang zirconium oxychloride ($ZrOCl_2.8H_2O$) precursor in accordance to the improved alkali fusion method by Subuki *et al.,* [19] using 6M NaOH and 8M HCl. Amang zirconium oxychloride solution was neutralized and hydrolyzed with ammonia until pH 10 to obtain zirconium hydroxide ($Zr(OH)_4$), ammonium chloride (NH_4Cl) and water according to the following reaction:

$$ZrOCl_2 .8H_2O + 2NH_4OH \rightarrow Zr(OH)_4 + 2NH_4Cl + 7H_2O \tag{2}$$
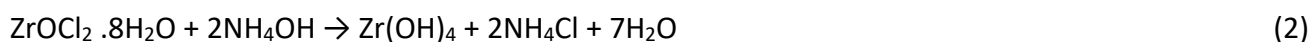
Next, zirconium hydroxide ($Zr(OH)_4$) obtained underwent vacuum filtration and washed with pure water and ethyl alcohol to remove chlorine and excess ammonia. The precipitate was left to dry at room temperature overnight. Then, zirconium hydroxide was calcined at varied temperature ranging from 400-800 °C for 4 hours to obtain high purity zirconia (ZrO_2) according to Eq. (3):

$$Zr(OH)_4 \rightarrow ZrO_2 + 2H_2O \tag{3}$$

2.3 Characterization

Zirconia powder was characterized to study the effect of calcination temperature on the synthesized zirconia powder. The elemental analysis was done on powdered zirconia using x-ray fluorescence (XRF) Malvern Panalytical Epsilon 3^{XLE}, from United Kingdom. X-Ray diffraction (XRD) Rigaku Ultima IV was used for phase analysis from range 10-80° with CuKα radiation and wavelength (λ) of 0.15 nm. Diffraction spectra was fixed with ICDD database and crystalline size was calculated with Scherrer formula

$$D = K\lambda/(\beta \cos \theta) \tag{4}$$

whereby D is the crystallite size, K is 0.9 Scherrer constant, λ is wavelength of CuKα radiation, θ is Bragg's angle and β is line broadening at half maximum. Scanning Electron Microscopy (SEM), Hitachi SU3500 was used to analyze the morphology and average particle size of the synthesized zirconia powder.

3. Results

This chapter described the results obtained from the elucidation study on effect of calcined temperature that had been carried out.

3.1 Elemental Analysis

Based on elemental composition analysis using x-ray fluorescence (XRF) in Table 1, 76.44 wt.% of zirconium and 1.80 wt.% silicon was recorded after zirconium oxychloride was hydrolyzed with ammonia to pH 10. Zirconium composition increased from 75.89 wt.% as zirconium hydroxide formed in accordance to Eq. (2) while silicon reduced because the precipitate was filtered and washed with

pure water and ethyl alcohol after decantation. Chlorine (Cl) was greatly removed to 0.08 wt.%. This indicated ammonium chloride (NH_4Cl) produced from the reaction was almost completely removed after being dissolved in pure water and ethyl alcohol. Other impurities reduced slightly or remained the same after hydrolyzed as the reaction only focused on the formation of zirconium hydroxide. However, neodymium (Nd) and thorium (Th) increased slightly due to the trace of monazite from unreacted Amang zircon sand.

Table 1
Elemental composition (wt.%) of zirconium powder

Element	$ZrOCl_2$	$Zr(OH)_4$
Zr	75.89	76.44
Si	1.83	1.80
Y	0.20	0.20
Hf	1.87	1.86
Fe	0.42	0.42
Ti	1.33	1.28
Cl	0.28	0.08
Ca	0.24	0.24
Ce	3.73	3.68
Nd	1.32	1.36
Th	0.82	0.96

In order to investigate the effect of temperature on zirconia powder synthesized from Amang zircon sand, zirconium hydrate powder was calcined at varied temperatures from 400-800 °C for 4 hours in order to obtain zirconia (ZrO_2) following Eq. (3). Based on the elemental analysis in Table 2, the highest zirconium dioxide (ZrO_2) was observed when calcined at 800 °C for 4 hours with value of 81.28 wt.% followed by calcined at 700 °C, 400 °C, 600 °C and 500 °C with readings of 74.90 wt.%, 74.51 wt.%, 66.13 wt.%, and 64.30 wt.% respectively. Zirconium oxide composition after calcination at 500 °C and 600 °C showed a slight decrease.

Typically, zirconia synthesized from decomposition of zircon showed a reduction in zirconium composition due to larger particle size. The average particle size of zirconium hydroxide before calcination process was rather large, which was approximately around 350 μm. Hence, the slight reduction of zirconium composition. The possible reason is that the larger particle size reduced the decomposition rate. On the other hand, the highest zirconium oxide obtained in this research was higher than in the previous study using Indonesia zircon sand. The study recorded a lower zirconium oxide at 72.07 wt.% [20].

Silicon dioxide (SiO_2) and yttrium oxide (Y_2O_3) were also present in the chemical composition analysis with values of 3.66 wt.% and 0.42 wt.% respectively at 800 °C. The adhesion of silicon and oxygen are stronger than other ions at lower temperature [21]. Hence, the formation of silicon dioxide actively increased throughout the process. As seen in Table 2, other elements increased together with formation of zirconium oxide. The impurities in the zirconium hydrate powder were not dissolved completely by ammonia. Besides, these impurities were also recorded in previous studies by using Indonesian and Australian zircon sand [21,22]. Research by Rahmawati *et al.,* [20] with Indonesian zircon sand managed to obtained a slightly lower silicon dioxide at 3.60 wt.% for zirconia calcined at 800 °C in a somewhat more prolonged duration of 5 hours.

It could be seen that cerium (Ce) and thorium (Th) increased to 4.40 wt.% and 1.03 wt.% respectively after calcined at 800 °C. These elements were extracted from a phosphate mineral monazite that existed in Amang zircon sand [12]. Chlorine (Cl) was found when calcined at 400 °C to 600 °C. However, this element decreased as the temperature increased and was completely absent

at 700 °C and 800 °C. This showed that ammonium chloride produced in Eq. (2) was completely melted during the calcination at higher temperature of 700 °C and 800 °C.

Iron (Fe) composition also increased after calcined at varied temperatures and the highest composition of iron was 0.80 wt.% after calcining at 800 °C. The composition doubled after calcination at 800 °C. Iron flakes were observed in the crucible after calcination due to the high calcine temperature used during the process.

Table 2
Elemental composition (wt.%) of Amang zirconia powder calcined at varied temperature

Element	400 °C	500 °C	600 °C	700 °C	800 °C
ZrO_2	74.51	64.30	66.13	74.90	81.28
SiO_2	3.56	3.12	3.09	3.45	3.66
Y_2O_3	0.4	0.36	0.36	0.4	0.42
Hf	2.24	1.97	2.02	2.27	2.40
Fe	0.76	0.68	0.72	0.78	0.80
Ti	1.16	1.13	0.92	1.27	0.97
Cl	0.14	0.09	0.07	-	-
Ca	0.22	0.19	0.20	0.22	0.24
Ce	4.59	4.06	4.08	4.72	4.40
La	-	-	1.80	-	1.97
Nd	1.47	1.32	1.20	1.51	1.26
Th	1.09	0.95	1.02	1.13	1.03

3.2 Phase Analysis

Based on the diffraction pattern in Figure 1, the peaks for Amang zirconia that were calcined at 400 °C were entirely dominated by monoclinic especially at the highest peak of 26.99° with crystallite size of 59.28 nm (ICDD 00-036-0420). The same was also observed by Prasad *et al.,* [23] using zirconyl nitrate precursor and Tyagi *et al.,* [24] using zirconium oxychloride precursor that was calcined at 400 °C. Monoclinic phase zirconia was also found at 28.14°, 38.51°, 53.44° and 55.59°. This showed that the zirconia calcined was almost purely monoclinic.

A minor tetragonal peak was found at 53.44° (ICDD 00-017-0923). It was worth noting that tetragonal phase appeared faster than previous study from India in which the tetragonal only appeared once the calcination reached 500 °C [23]. This showed that the proposed method in this study achieved a faster phase transformation from monoclinic to tetragonal phase at a lower temperature. The presence of tetragonal at 400 °C was also reported by Torres-GarciÁa *et al.,* [25], by using almost the same method as proposed. The faster phase transformation rate signified an improved heat transfer during reaction, which was attained from the deagglomeration, and large surface area of 0.319 m^2/g compared to 0.039 m^2/g from before calcination. This was supported by the particle size reduction from 350 µm after ammonia hydrolysis to 143 µm due to the deagglomeration. Leib *et al.,* [26] also reported the formation of tetragonal starting at 450 °C.

The highest peak of 28.23° was determined to be monoclinic zirconium after calcined at 500 °C (ICDD 00-036-0420). Monoclinic zirconium could be found in several other peaks at 35.65°, 53.43°, 55.61°, 59.75° and 62.90°. Other phases of zirconium were also detected. Tetragonal zirconium could be found at 35.65° (ICDD 00-002-0733). Yttrium (Y) was also detected at this peak. Tetragonal was also available at 59.75° alongside monoclinic zirconia. The presence of tetragonal was slightly abundant compared to the previous pattern at 400 °C. This was probably because of the increased temperature, and it favored the formation of tetragonal zirconium. This also showed that phase

transformation of monoclinic and tetragonal already occurred. The crystallite size was recorded at 60.12 nm. The peaks were also sharper. This indicated that the crystalline nature of the sample was increasing [4].

Zirconia powder calcined at 600 °C has a high monoclinic zirconium peak of 26.98°. The same phase of monoclinic zirconium was also detected at 28.25°, 30.23°, 38.47°, and 55.59° (ICDD 00-024-1165). Three phases of zirconium were found at 30.23°, namely monoclinic, tetragonal, and cubic. Note that cubic phase was only found in a single peak compared to monoclinic and tetragonal phase. Cubic zirconia was observed by Manivasakan *et al.,* [27] earlier at 500 °C with zirconium hydroxide precipitated from pH 10. This shows that it was possible to obtain cubic zirconia at low temperature. However, the calcination time was insufficient to calcine cubic zirconium as Manivasakan *et al.,* [27] reported to calcine zirconia powder for 6 hours in order to obtain a small cubic peak.

Yttria was detected at a minor peak of 43.77° alongside silicon (ICDD 01-074-1828). Silicon was also detected to coexist at 28.25° and 55.59° with monoclinic zirconium. The crystallite size was calculated at 82.08 nm which was higher compared to the crystallite size at 500 °C. Besides, it was reported that 600 °C was the threshold temperature for tetragonal zirconia formation [23]. Monoclinic phase increased as the temperature increased. Thus, the crystallite size increased from 60.12 nm at 500 °C to 82.08 nm at 600 °C.

At calcination of 700 °C, the highest peak of 26.87° belongs to monoclinic with crystallite size of 41.43 nm. As with previous patterns, monoclinic zirconium could be found in other peaks at 27.99°, 30.14°, 35.45°, 50.32°, 55.51° and 60.18°. At peaks 27.99° and 55.51°, silicon was also detected alongside monoclinic zirconium. Monoclinic, tetragonal, and cubic zirconium were found together at 30.14°, 35.45°, 50.32°, and 60.18°. Yttrium could also be found at 35.45°, 50.32°, and 60.18° alongside all three zirconium phases.

According to Prasad *et al.,* [23], zirconia exists in either monoclinic or cubic phase above the threshold temperature of tetragonal formation as it was almost impossible to achieve a metastable tetragonal due to the heat transfer in the system. It was reported that the initial monoclinic started as the temperature increased but the sample transformed to monoclinic entirely due to the crystallite size being bigger than the critical size [27]. The crystallite size also reduced from 82.08 nm to 41.43 nm. This reduction of crystallite size hindered the phase transformation of cubic to tetragonal phase zirconia. This cubic to tetragonal transformation favored higher crystallite size in high calcination temperatures. Consequently, monoclinic, and cubic zirconia formation at 700 °C were notably higher than previously at 600 °C.

According to the diffraction pattern in Figure 1, monoclinic zirconium was found at the highest peak of 26.88° after being calcined at 800 °C. Peaks 28.12°, 30.07°, 35.20°, 38.42°, 50.23°, 55.48°, 60.17°, and 62.78° contained monoclinic zirconium. Tetragonal and cubic zirconium could be found at 30.07°, 35.20°, 50.23°, 60.17°, and 62.78° alongside with monoclinic zirconium. A minor silicon could be found at 55.48° with monoclinic zirconium. At 73.24°, only tetragonal zirconium and yttrium were detected. The crystallite size was calculated at 74.22 nm which increased from 41.43 nm at 700 °C. The increment of crystallite size at 800 °C after reduction at 700 °C, showed that tetragonal phase in the sample increased [24]. Thus, the tetragonal peak at 30.07° increased significantly compared to temperature below 700 °C.

It could be seen that the highest peaks at every temperature from 400-800 °C were predominantly monoclinic zirconium which was thermodynamically stable phase than other two phases [31]. The same monoclinic pattern was observed by Wilk *et al.,* [29] and Ramachandran *et al.,* [30]. It was observed that the diffraction line became sharper and narrower as the calcination temperature increased. The sharp and narrow peaks indicated the formation of larger crystallite [4]. The dominant monoclinic phase was due to the temperature which was still in the phase

transformation threshold and it was expected as there was no addition of dopant in the zirconia [31]. Besides, it also showed that the sintering temperature was not high enough to stabilize and transition a metastable tetragonal zirconia. The formation of tetragonal phase increased along with substantial amount of monoclinic phase [24].

On the other hand, the temperature was sufficient to initiate a certain level of tetragonal phase transformation from the monoclinic phase. This could be observed by the increasing presence of tetragonal phase at peak 30.07° (ICDD 00-017-0923) due to the progressive phase transformation as the temperature increased. The same could also be observed for cubic zirconium phase from the cluttered peaks starting at 700 °C. This cluttered and disorderly crystallite patterns in varying degree was ascribed to the high degree of thermal vibration between crystals at high temperature.

It was also worth noting that the highest peak of monoclinic zirconium in every calcination from 400-800 °C reduced as the temperature increased. This was due to the transition formation of other tetragonal and cubic zirconium phases. Tetragonal peaks were also broader and more defined as the temperature increased. This phenomenon was also recorded by Prasad *et al.,* [23]. The intensity of tetragonal when calcined at 800 °C was higher compared to the other temperature and the corresponding peak when calcined at 700 °C was slightly weaker compared to 800 °C.

From the diffractogram pattern, a minor broadened tetragonal crystal peak 30.07° started at 400 °C. The broad peak indicated a lower and finer crystallinity of tetragonal. This may be attributed by the high pH 10. High pH increased the interaction between ammonia hydroxide and zirconium and influenced the crystal size during the reaction process. Crystallite size less than 100 nm was observed throughout the synthesizing process of zirconia from Amang precursor. According to literature, the increase of crystallite size influenced the phase transformation of tetragonal zirconia [27]. Thus, the highest crystallite size of 82.08 nm at 600 °C has the highest tetragonal phase.
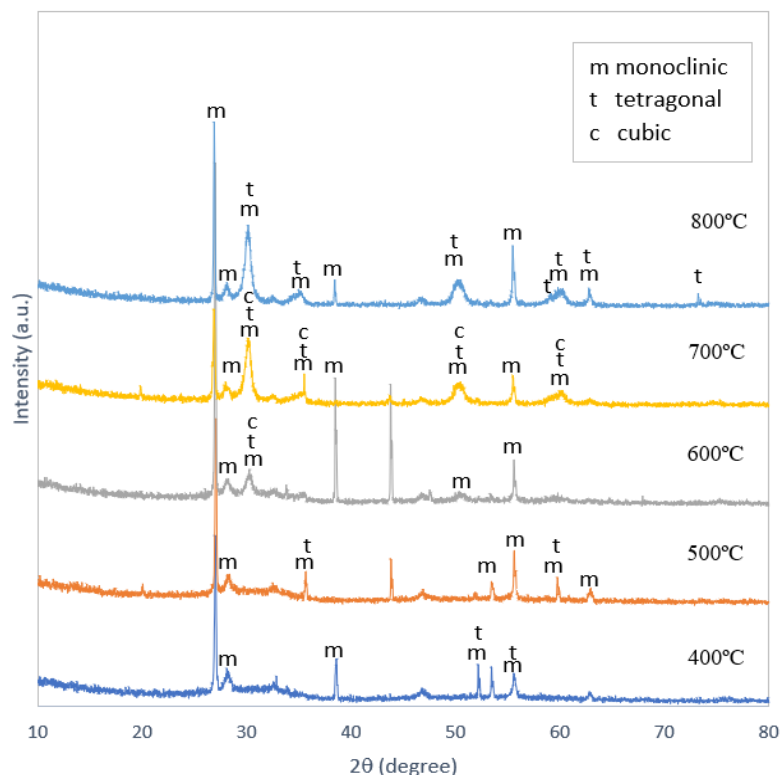

Fig. 1. XRD pattern Amang zirconia powder calcined in varied temperature

The increase in crystallite size was also reported by Leib *et al.,* [26] at 850 °C using zirconium tetrachloride (ZrCl$_4$) precursor in which they justified it as in accordance to the phase transformation of tetragonal to monoclinic. According to the literature, the transformation was accompanied by volume expansion of 3-5% [22,31]. Their research also reported that phase transformation increased significantly once the temperature rose above 650 °C.

3.3 Morphology Analysis

The morphology analysis of synthesized zirconia was obtained by using scanning electron microscopy (SEM). A very small amount of powder was scattered on a carbon covered stub and coated with gold layer. This procedure was standardized and done on all samples. According to the morphological analysis with the magnification of 1,000X in Figure 2, irregular angular and pyramidal shape in various grain sizes was detected in Amang zirconia powder calcined at 400 °C. As the temperature increased until 800 °C, the crystals were almost indiscernible. The crystal size at every temperature ranged from 8-30 μm, which was rather large due to the agglomeration of powder. Ramachandran *et al.,* [30] explained that the agglomeration of monoclinic zirconia occurred quickly due to the strong Van-der-walls force between particles.
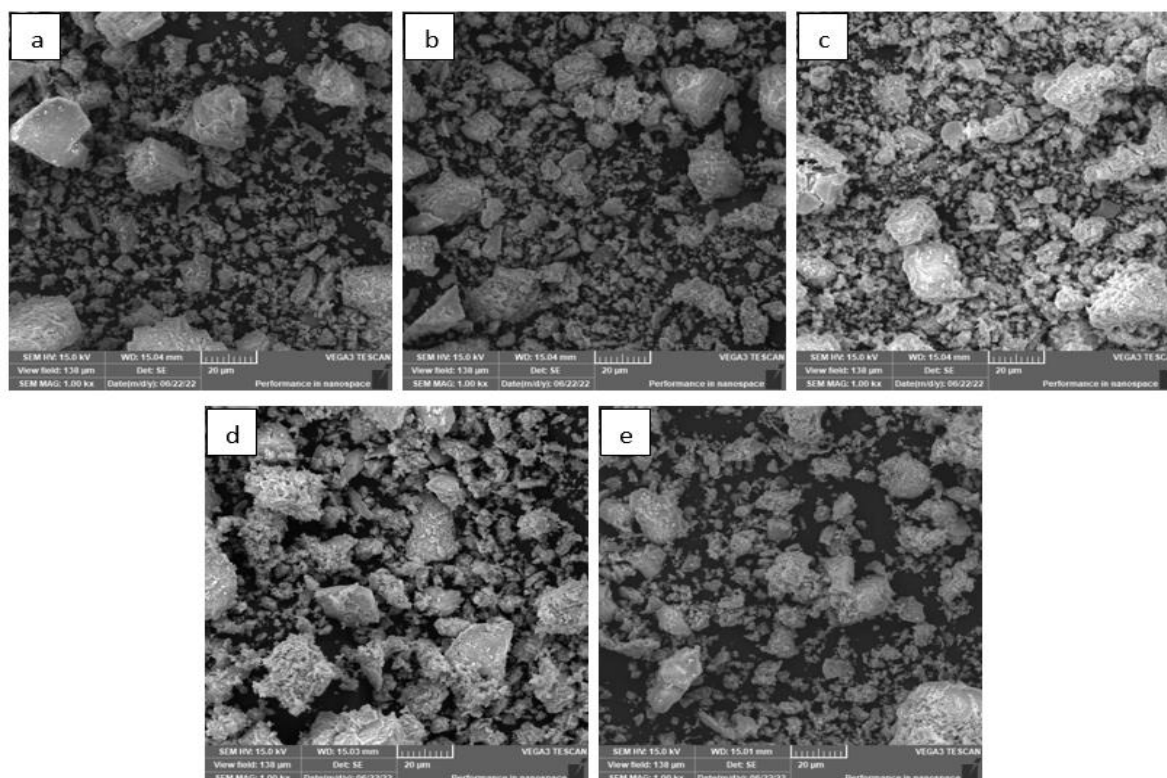

Fig. 2. SEM photography of zirconia at (a) 400 °C, (b) 500 °C, (c) 600 °C, (d) 700 °C, and (e) 800 °C

Particle attrition was also observed starting at 700 °C and it was even more evident in 800 °C when analyzed under higher magnification as seen in Figure 3. This was due to the reaction that usually occurred on the particle surface [17]. This might be related to particle size reduction compared to other temperatures.
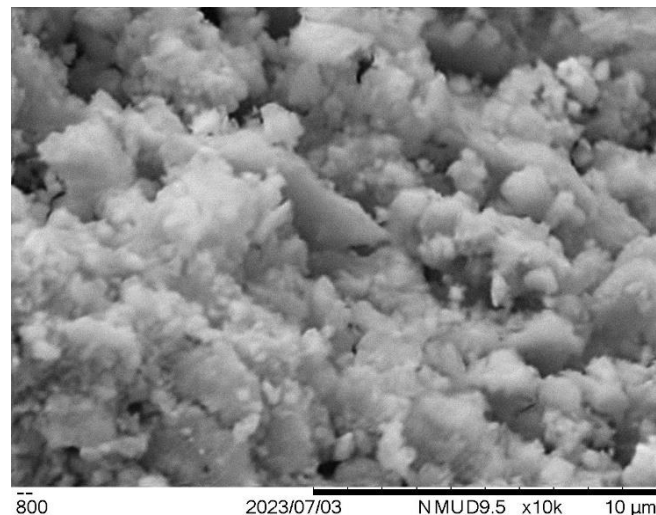
Fig. 3. SEM photography of zirconia at 800 °C (10,000X)

4. Conclusions

Based on the finding, monoclinic zirconia powder with a small fraction of tetragonal and cubic phase was successfully synthesized from Amang zirconium oxychloride precursor with an improved alkali fusion method using 6M sodium hydroxide (NaOH) and 8M hydrochloric acid (HCl). It was also established that temperature did influence the formation of zirconium oxide in which the highest zirconium composition was recorded at 81.28 wt.% when calcined at 800 °C. In contrast, the lowest was calcined at 400 °C with 74.51 wt.%. The chemical composition of zirconium showed increment alongside calcination temperature. The formation of silicon dioxide was also considered as low at only 3.66 wt.%. High composition of zirconium with low impurities after calcination was a good indication of suitability using Amang precursor to synthesize zirconia powder. Particle size reduction was also seen at higher temperature of 700 °C and more apparent at 800 °C, which led to increase of zirconium composition. Therefore, 800 °C was deemed the best calcination temperature to obtain a higher zirconium composition with relatively low impurities for zirconia powder synthesized from Amang zirconium oxychloride precursor.

References
[1] Xu, Xiaohong, Ao Li, Jianfeng Wu, Yongqi Yin, Sitong Ma, and Jiajun Yuan. "Effect of zirconia addition amount in glaze on mechanical properties of porcelain slabs." *Ceramics International* 49, no. 12 (2023): 20080-20087. https://doi.org/10.1016/j.ceramint.2023.03.131
[2] Sultana, N., K. Bilkis, R. Azad, M. R. Qadir, M. A. Gafur, and M. Z. Alam. "Yttria stabilized tetragonal zirconia ceramics: preparation, characterization and applications." *Bangladesh Journal of Scientific and Industrial Research* 53, no. 2 (2018): 111-116. https://doi.org/10.3329/bjsir.v53i2.36671
[3] Soni, Dimple, Jaiveer Singh, Netram Kaurav, Jitendra Tripathi, and Anupam Sharma. "Synthesis and characterization of zirconia nanocrystalline powder by thermal treatment method." *Materials Today: Proceedings* 54 (2022): 908-911. https://doi.org/10.1016/j.matpr.2021.11.219
[4] Baba, Nor Bahiyah, Amirul Syazwan Ghazali, Afifah Humaira Abdul Rahman, Nor Azinee Said, and Safian Sharif. "Influence of Heat Treatment on Microhardness and Surface Roughness of Electroless Ni-YSZ Composite Coating." *Journal of Advanced Research in Fluid Mechanics and Thermal Sciences* 99, no. 1 (2022): 114-122.

https://doi.org/10.37934/arfmts.99.1.114122

[5]   Murti, C. F. K., U. Maslakah, E. Endarko, and T. Triwikantoro. "Structural, physical and mechanical properties of zirconia-polymorph/alumina composites." *Materials Chemistry and Physics* 285 (2022): 126102. https://doi.org/10.1016/j.matchemphys.2022.126102

[6]   Norman, Nur Wardah, Mahendra Rao Somalu, and Andanastuti Muchtar. "A Short Review on the Proton Conducting Electrolytes for Solid Oxide Fuel Cell Applications." *Journal of Advanced Research in Fluid Mechanics and Thermal Sciences* 52, no. 2 (2018): 115-122.

[7]   Guo, Mingyi, Guangxin Wang, Yunchao Zhao, Haitao Li, Kun Tang, Yibo Zhao, and Kevin Burgess. "Preparation of Nano-ZrO_2 powder via a microwave-assisted hydrothermal method." *Ceramics International* 47, no. 9 (2021): 12425-12432. https://doi.org/10.1016/j.ceramint.2021.01.099

[8]   Ranjbar, M., M. Yousefi, M. Lahooti, and A. Malekzadeh. "Preparation and characterization of tetragonal zirconium oxide nanocrystals from isophthalic acid-zirconium (IV) nanocomposite as a new precursor." *International Journal of Nanoscience and Nanotechnology* 8, no. 4 (2012): 191-196.

[9]   Davar, Fatemeh, and Mohammad Reza Loghman-Estarki. "Synthesis and optical properties of pure monoclinic zirconia nanosheets by a new precursor." *Ceramics International* 40, no. 6 (2014): 8427-8433. https://doi.org/10.1016/j.ceramint.2014.01.052

[10]   Keerthana, L., C. Sakthivel, and I. Prabha. "MgO-ZrO_2 mixed nanocomposites: fabrication methods and applications." *Materials Today Sustainability* 3 (2019): 100007. https://doi.org/10.1016/j.mtsust.2019.100007

[11]   Abi, C. B. Emrullahoglu. "Toughening mechanisms in dental composites." *Toughening Mechanisms in Composite Materials* (2015): 321-337. https://doi.org/10.1016/B978-1-78242-279-2.00012-3

[12]   Blanchart, Philippe. "Extraction, Properties and Applications of Zirconia." *Industrial Chemistry of Oxides for Emerging Applications* (2018): 165-209. https://doi.org/10.1002/9781119424079.ch4

[13]   13Gauna, Matías Roberto, María Susana Conconi, Sofía Gómez, Gustavo Suárez, Esteban Fausto Aglietti, and Nicolás Maximiliano Rendtorff Birrer. "Monoclinic-Tetragonal Zirconia quantification of commercial nanopowder mixtures by XRD and DTA." *Ceramics-Silikáty* 59, no. 4 (2015): 318-325.

[14]   14Hamzah, Zaini, Nor Monica Ahmad, and Ahmad Saat. "Determinion of heavy minerals in amang from Kampung Gajah ex-mining area." *Malaysian Journal of Analytical Sciences* 13, no. 2 (2009): 194-203.

[15]   15Kumar, P., M. Nath, A. Ghosh, and Himansu Sekhar Tripathi. "Enhancement of thermal shock resistance of reaction sintered mullite-zirconia composites in the presence of lanthanum oxide." *Materials Characterization* 101 (2015): 34-39. https://doi.org/10.1016/j.matchar.2015.01.004

[16]   16Yustanti, E., F. A. F. Ode, and E. Sulistiyono. "Primary study of KOH alkali fusion-nitric acid leaching process in extraction of West Kalimantan zircon concentrate." In *IOP Conference Series: Materials Science and Engineering*, vol. 763, no. 1, p. 012065. IOP Publishing, 2020. https://doi.org/10.1088/1757-899X/763/1/012065

[17]   17Sun, Hong-qian, Song Jing, Sun Shuai, Jing-kui Qu, Lü Wei, and Qi Tao. "Decomposition kinetics of zircon sand in NaOH sub-molten salt solution." *Transactions of Nonferrous Metals Society of China* 29, no. 9 (2019): 1948-1955. https://doi.org/10.1016/S1003-6326(19)65102-2

[18]   18Lestari, Novia Dwi, Rizka Nurlaila, Nibras Fuadi Muwwaqor, and Suminar Pratapa. "Synthesis of high-purity zircon, zirconia, and silica nanopowders from local zircon sand." *Ceramics International* 45, no. 6 (2019): 6639-6647. https://doi.org/10.1016/j.ceramint.2018.12.152

[19]   19Subuki, I., N. F. F. Norsham, N. A. Mahayuddin, and Q. M. Ali. "Influence on Ratio of NaOH/$ZrSiO_4$ in Alkali Fusion for Amang Zircon Sand." *ASM Science Journal* 17 (2022). https://doi.org/10.32802/asmscj.2022.1093

[20]   20Rahmawati, Fitria, Ita Permadani, Syoni Soepriyanto, Dani Syarif, and Eddy Heraldy. "Double steps leaching and filtration in caustic fusion method to produce zirconia from local zircon concentrate." In *2014 International Conference on Physics and its Applications (ICOPIA-14)*, pp. 99-102. Atlantis Press, 2014. https://doi.org/10.2991/icopia-14.2015.18

[21]   21He, Bei, Guang Xu, Mingxing Zhou, and Qing Yuan. "Effect of oxidation temperature on the oxidation process of silicon-containing steel." *Metals* 6, no. 6 (2016): 137. https://doi.org/10.3390/met6060137

[22]   22Kelly, J. Robert, and Isabelle Denry. "Stabilized zirconia as a structural ceramic: an overview." *Dental Materials* 24, no. 3 (2008): 289-298. https://doi.org/10.1016/j.dental.2007.05.005

[23]   23Prasad, Krishnamurthy, D. V. Pinjari, A. B. Pandit, and S. T. Mhaske. "Synthesis of zirconium dioxide by ultrasound assisted precipitation: effect of calcination temperature." *Ultrasonics Sonochemistry* 18, no. 5 (2011): 1128-1137. https://doi.org/10.1016/j.ultsonch.2011.03.001

[24]   24Tyagi, Beena, Kalpesh Sidhpuria, Basha Shaik, and Raksh Vir Jasra. "Synthesis of nanocrystalline zirconia using sol−gel and precipitation techniques." *Industrial & Engineering Chemistry Research* 45, no. 25 (2006): 8643-8650. https://doi.org/10.1021/ie060519p

[25]   25Torres-GarciÁa, E., A. Peláiz-Barranco, C. Vázquez-Ramos, and G. A. Fuentes. "Thermal and structural characterization of the $ZrO_{2-x}(OH)_{2x}$ to ZrO_2 transition." *Journal of Materials Research* 16, no. 8 (2001): 2209-2212.

https://doi.org/10.1557/JMR.2001.0303

[26] 26Leib, Elisabeth W., Ulla Vainio, Robert M. Pasquarelli, Jonas Kus, Christian Czaschke, Nils Walter, Rolf Janssen et al. "Synthesis and thermal stability of zirconia and yttria-stabilized zirconia microspheres." *Journal of Colloid and Interface Science* 448 (2015): 582-592. https://doi.org/10.1016/j.jcis.2015.02.049

[27] 27Manivasakan, Palanisamy, Venkatachalam Rajendran, Prema Ranjan Rauta, Bhakta Bandhu Sahu, and Bharati Krushna Panda. "Synthesis of monoclinic and cubic ZrO_2 nanoparticles from zircon." *Journal of the American Ceramic Society* 94, no. 5 (2011): 1410-1420. https://doi.org/10.1111/j.1551-2916.2010.04277.x

[28] 28Mokhtar, Mohamed, Sulaiman N. Basahel, and Tarek T. Ali. "Effect of synthesis methods for mesoporous zirconia on its structural and textural properties." *Journal of Materials Science* 48 (2013): 2705-2713. https://doi.org/10.1007/s10853-012-7068-9

[29] 29Wilk, Agnieszka, Kamil Wojteczko, Marta Gajewska, Radosław Lach, Piotr Jeleń, Maciej Sitarz, Krzysztof Haberko, and Zbigniew Pędzich. "Effect of Y_2O_3 additive on morphology and phase composition of zirconia solid solutions." *Ceramics International* 48, no. 9 (2022): 13055-13062. https://doi.org/10.1016/j.ceramint.2022.01.180

[30] 30Ramachandran, M., R. Subadevi, Wei-Ren Liu, and M. Sivakumar. "Facile synthesis and characterization of ZrO_2 nanoparticles via modified co-precipitation method." *Journal of Nanoscience and Nanotechnology* 18, no. 1 (2018): 368-373. https://doi.org/10.1166/jnn.2018.14562

[31] 31Prakasam, Mythili, Sorina Valsan, Yiying Lu, Félix Balima, Wenzhong Lu, Radu Piticescu, and Alain Largeteau. "Nanostructured pure and doped zirconia: syntheses and sintering for SOFC and optical applications." *Sintering Technology-Method and Application* 85 (2018): 85-105. https://doi.org/10.5772/intechopen.81323